Journal of Physical Science, Vol. 34(1), 87–108, 2023

Mechanical and Corrosion Protection Characteristics of CNTs/epoxy resin Nanocomposite Coating on Buried API 5L X65 Steel Storage Tank

Aliyu Shehu Buhari,[1] Asipita Salawu Abdulrahman,[2] Sunday Albert Lawal,[1] Ambali Saka Abdulkareem[3] Rasheed Aremu Muriana,[2] Oladejo Tijani Jimoh,[4] Hassan Kobe Ibrahim[1,5] and Yusuf Olanrewaju Busari[6,7*]

[1]Department of Mechanical Engineering, Federal University of Technology Minna, P. M.B. 65, 920101, Nigeria
[2]Department of Material and Metallurgical Engineering, Federal University of Technology Minna, P.M.B. 65, 920101, Nigeria
[3]Department of Chemical Engineering, Federal University of Technology Minna, P.M.B. 65, 920101, Nigeria
[4]Department of Chemistry, Federal University of Technology Minna, P.M.B. 65, 920101, Nigeria
[5]Department of Mechanical Engineering, University of Ilorin, P.M.B 1515, 240003 Ilorin Nigeria
[6]Department of Material and Metallurgical Engineering, University of Ilorin, P.M.B 1515, 240003 Ilorin, Nigeria
[7]School of Mechanical Engineering, Universiti Teknologi MARA, 40450 Shah Alam, Selangor, Malaysia

[*]Corresponding author: busari.oy@unilorin.edu.ng

Published online: 28 April 2023

To cite this article: Buhari, A. S. et al. (2023). Mechanical and corrosion protection characteristics of CNTs/epoxy resin nanocomposite coating on buried API 5L X65 steel storage tank. *J. Phys. Sci.*, 34(1), 87–108. https://doi.org/10.21315/jps2023.34.1.8

To link to this article: https://doi.org/10.21315/jps2023.34.1.8

ABSTRACT: *The storage of petroleum products in buried metal tanks to ensure safety is common practice. However, the integrity of these tanks could be compromised by soil corrosion with economic and environmental consequences. This study examines carbon nanotubes mechanical and anti-corrosive capabilities (CNTs) and epoxy resin coating on steel tanks. The presence of corrosive ions, resistivity, and pH values were all tested in the soil sample. CNT was mixed in proportions of 1.5, 2.5, 3.5 and 4.5 weight percent of epoxy resin to create the coatings. The morphology of uncoated steel, epoxy, and CNTs/epoxy resin-coated steel specimens was studied using high-resolution scanning electron microscopy (HRSEM) equipment with energy dispersive x-ray spectroscopy (EDX). Electrochemical impedance spectroscopy (EIS) was used for corrosion analysis, and*

© Penerbit Universiti Sains Malaysia, 2022. This work is licensed under the terms of the Creative Commons Attribution (CC BY) (http://creativecommons.org/licenses/by/4.0/).

the morphological result was established. The average ions content soil samples showed 272 mg/kg chloride, 467.20 mg/kg sulphate and 167.40 Ω-m for the average resistivity value. The sample's pH was acidic because it fell within 6.11–7.48. The tensile strength, hardness, and tensile modulus of epoxy resin with CNTs increase with CNTs. The addition of 3.5% CNTs has the best effect on the mechanical strength of the composite. The nanocomposite coatings exhibited considerably superior conductors, according to the EIS investigation. Thus, the hybrid of epoxy and CNTs increases the hydrophobicity of the coated surface.

Keywords: coating, corrosion, carbon nanotubes, steel tank, nanocomposite

1. INTRODUCTION

The storage tanks for petroleum products are usually made of steel, either elevated or buried for gravity and safety reasons. The corrosive ions or fluids in the soil encourages underground storage tanks to corrode.[1] This phenomenon reduces the strength, appearance and permeability to liquids and gases of steel materials and structures.[2] The pH value, salt content, conductivity, carbon dioxide partial pressure, organic acid content and temperature are crucial in exacerbating corrosion. Hence, the pH is a key factor in soil corrosion mechanisms.[3] Various corrosion treatment procedures, such as anodisation, metal plating and organic coating, have been used to protect metallic substrates. Paint and anti-corrosive coatings are the most common and cost-effective treatments utilised regularly.[4] Three main protection mechanisms are barrier protection, passivation and sacrificial protection.[5]

Water molecules at the coating substrate contact may cause electrochemical corrosion of the metal beneath the coating, reducing coating adherence. Consequently, adding inorganic (polymeric) additives to the coating effectively improves coating permeability.[6] Epoxy resin is one of the most flexible and competitive materials for constructing composites, owing to its exceptional qualities of strong adhesion strength, easy processing, high modulus and thermal stability. Meanwhile, the high crosslinking density of epoxy reduces toughness and impact resistance, resulting in a very brittle structure with poor hindrance towards fracture initiation and propagation.[7] The porosity and low adherence of epoxy resins are the fundamental flaws that prevent them from being widely used. This includes rubbers, particles have proven to be an effective approach to increasing toughness but lowering thermal stability and mechanical strength.[8]

Many efforts have recently been made to improve the efficiency of epoxy coatings by introducing nanoparticles such as nano silica, nano clay, carbon nanotubes (CNTs) and graphene platelets into the formulation.[9,10] Carbon nanofillers reinforced epoxy composites have been shown to significantly enhance the toughness of corrosion-resistant applications to meet the high demands on mechanical qualities.[11] Because of their structure-dependent tunable features, such as mild chemical stability, high electrical conductivity and excellent thermal conductivity carbon-based nanomaterials have gotten a lot of interest in the last two decades.[12] These CNTs have been widely studied in corrosion protection applications, both theoretically and empirically. Alishahi et al. prepared and evaluated the corrosion resistance of electroless nickle-phospurus-CNT (Ni-P-CNT) composite coatings with various CNTs.[13] In a 3.5% sodium chloride (NaCl) aqueous solution at room temperature, the corrosion behaviour of the coatings was measured using Tafel polarisation and electrochemical impedance spectroscopy (EIS). When compared to Ni-P coatings, the results showed that Ni–P–CNT composite coatings had superior passivation and corrosion resistance.

The impact of CNTs on the mechanical properties and corrosion behaviour of mild steel in an acidic environment under various coating circumstances medium was evaluated. The mechanical parameter values of coated steel samples improved as the coating temperature and holding time were increased. When comparing the different coating circumstances, coated steels at 950°C for 90 min showed higher hardness, yield strength, and tensile strength values than others. In addition, with increased holding time and coating temperature, the corrosion current and rate of the coated steel samples dropped.[14] Also, the corrosion behaviour of electrodeposited Ni, Ni-aluminium oxide (Al_2O_3), Ni-zirconium dioxide (ZrO_2) and Ni-graphene (Gr) coatings in a moist sulphur dioxide (SO_2) environment was examined. Nano indentation tests revealed that Ni-Al_2O_3, Ni-ZrO_2 and Ni-Gr nanocomposite coatings have higher mean hardness and elastic modulus than pure Ni coatings.[15] The increased mechanical properties of nanocomposite coatings can improve the coating's durability and applicability. Based on the smaller scratch depth, the nanocomposite coatings offer a stronger wall.

Janaki and Xavier investigated the effect of indole functionalised nano-alumina on the corrosion protection performance of epoxy coatings in the marine environment.[16] In a continuous aqueous environment, the coated steel substrate produces iron oxide (Fe_3O_4), which was found in 38.5% of the time. X-ray diffraction analysis (XRD) examination of a 40-day immersion sample reveals the presence of Fe_3O_4 in the top layer of rust. In the corrosion products, Fe, Al, O and N are confirmed by the energy dispersive x-ray spectroscopy (EDX) analysis. After a one-day immersion, the functionalised alumina nanocomposite exhibits uniform matrix dispersion in the field emission scanning electron microscopy (FE-SEM). The pure epoxy-coated samples had a hardness value of 95 MPa after 40 days, while epoxyindole/alumina nanocomposite-coated samples had a hardness value of

680 MPa after 40 days. The epoxyindole/alumina nanocomposite-coated sample had a higher coating hardness, indicating decreased porosity. Based on recent reports, the anti-corrosion behaviour of nanocomposite coatings has not been exhaustively studied. Moreso, the creation of acidic soil due to acid rain or the reaction between moisture and dry chlorine and sulfur deposits makes the understanding of how ions induce corrosion in actual scenarios like buried tanks and pipes necessary. This study aims to examine the morphological, mechanical and corrosion behaviour of coatings on the buried tank in the soil with variable levels of chloride, sulphate, resistivity, temperature and pH in other to develop a sustainable environment. The synthesis of CNT/epoxy resin nanocomposite as coatings on mild steel has been carried out.

2. MATERIALS AND METHOD

The API 5L X65 steel obtained from steel market in Minna, Niger State, Nigeria is washed thoroughly with acetone (97%) to remove grease, dirt, oil, oxide, and protective layers. All the steel samples were weighed using the digital weighing balance. The vernier caliper was used to measure the thickness with (100 x 100 x 8) mm dimensions and labeled for easier identification. The round sieve is set to receive coated steel samples for curing. The chemical composition of the steel used is determined with optical emission spectroscopic (OES) analysis (SpectroMaxx LMF06, Agilent Scientific Instruments, United States) and verified with the standard maximum value of main element composition as illustrated in Table 1.

Table 1: Specimen chemical composition.

Elements (wt%)	C	Mn	P	S	Si	Cr	Mo	Ni	Cu	Vn	Fe
	0.26 max	1.45 max	0.03 max	0.03 max							
Specimen	0.06	1.015	0.02	0.01	0.28	0.03	0.013	0.45	0.2	0.06	Bal.

2.1 Nanoparticles Catalyst Production

Chemicals with (99%) purity of cobalt(II) nitrate hexahydrate [$Co(NO_3)_2.6H_2O$] and Molybdenum(II) Nitrate hexahydrate [$Mo(NO_3)_2.6H_2O$] were obtained from Kem Light Lab. Mumbai, India and magnesium oxide (MgO) was obtained from Kermel, China. The wet impregnation method is used to synthesise cobalt-molybdenum (1:1) (Co-Mo) supported on MgO. Approximately 19.4 g $Co(NO_3)_2.6H_2O$ and 1.2 g Mo $(NO_3)_2.6H_2O$ salts were dissolved in 50 cm^3 of purified water. After allowing the mixture to dissolve completely, 15 g of MgO is added. The mixture is agitated for 1 h at 1500 rpm using a magnetic stirrer as reported in literature.[17,18] The resulting slurry is then dried in an oven at 115°C for 11 h. The dried catalyst is crushed and sieved through 150 μm sieve aperture to acquire homogeneous particle sizes. The uniformly sieved catalyst is then calcined in an electric furnace for 2 h to 4 h at temperature between 500°C and 600°C.

2.2 Synthesis of CNTs

A horizontal Chemical Vapour Deposition (CVD) reactor synthesised the CNTs, 0.5 g of the produced Co-Mo/MgO catalyst is placed in the quartz reactor's core. The reactor is purged with nitrogen gas at 50 ml/min rate until the reaction temperature reached 700°C. This temperature increases the nitrogen flow rate to 200 ml/min while the acetylene flow rate is released for the carbon nucleation process during an hour reaction time as demonstrated by Lobiak, V. E. et al.[19] When the reaction time was reached, the acetylene flow was truncated, and the nitrogen flow is reduced to 50 ml/min until the system reached room temperature. Next, the boat containing the carbon nanotubes is removed and weighed to determine the CNTs' percentage yield. The CNTs were found in a clump softly mashed to particles with a ceramic mortar and pestle. The surface area, surface morphology, crystallinity and surface functional group of the resulting CNT were then investigated using Brunauer, Emmett and Teller analyser, scanning electron microscope (SEM), XRD and fourier transform infrared (FTIR) techniques.

2.3 Production of Epoxy Resin and CNTs Coating Substrates

The epoxy resin material is mixed with synthesised multi-walled CNTs(MWCNT) in 1.5, 2.5, 3.5 and 4.5 proportions, using the density of the mixture magnetic stirrer to the obtained black precipitate slurry of epoxy and CNT mixture as conducted by Raza et al.[20] The prepared steel samples were dipped into the slurry one by one for 10 s each, then coated steel samples from the slurry were removed with the aid of a picker and placed on the smooth surface, and dried for three days. The coating and drying were repeated three times to increase the slurry loading on the steel sample to get the required thickness of 2.5 mm, obtained with a Minifest coating thickness digital meter according to Sigma Coating Standard. The experimental selection, coated epoxy resin, and mixture (epoxy resin and

MWCNT) of 98.5:1.5, 97.5:2.5, 96.5:3.5 and 95.5:4.5. The coated steel substrates were left in the laboratory to cure at room temperature.

2.4 Characterisation of the Experimental Specimens

The soil samples were collected from five different areas at the Federal University of Technology, Minna (9.5836° N, 6.5463° E) to carry out the morphology of corroded samples. The soil was characterised for ions and moisture content, pH, and resistivity values according to methods of test for Soils for civil engineering purposes BS1377-3:1990 (BSI, 1990a and 1990b) and standard test method for measurement of soil resistivity ASTM (G57) respectively. The uncoated, epoxy-coated, and nanocomposite-coated steel substrates were buried for 3, 6, 9 and 12 months in five pits with 1.5 m depth. The corrosion samples' chemical composition and surface morphology were examined using high-resolution scanning electron microscopy (HRSEM) equipped with EDX. The mechanical properties of the coated steel were measured using the tensile and hardness tests. The tensile properties of the samples were determined on rectangular shaped pieces of 80 mm x 12 mm x 3 mm with a cross-head speed of 1 mm/min at room temperature with Servo-control system universal testing machine with U60 testing software (AI-7000 series, Gotech Testing Machines Inc, Taiwan). The ultimate tensile strength and modulus of elasticity were calculated using the load-extension data on the generated graph sheet and the sample specifications. The surface microhardness values of the steel samples were determined using the Vickers microhardness test (HMV-2000, Shimadzu, Japan). The treated samples surfaces were subjected to a compressive load of 1.96 N for 15 s with a square-based pyramid and a 136° angle between opposite faces (d_1 and d_2). The average of three measurements was used to determine the microhardness of the treated materials and the control sample. The Vickers hardness (HV) was computed using Equation 1:[14]

$$HV = \frac{2 \cdot F \cdot \sin 68^\circ}{D^2} \tag{1}$$

where,

F = the applied force (N)

D = the mean diagonal of the indentation as $D = \frac{d1 + d2}{2}$ in mm.

Corrosion evaluation was conducted using EIS tests at 38^{o}C temperature was obtained in the soil test. The standard three-electrode cell uses a platinum electrode and Saturated Calomel Electrode (SCE) as auxiliary and reference electrodes, respectively, as described by Isakhani-Zakaria et al.[21] EIS was measured using a Solartron Model SI1255A-HF Frequency Response Analyser connected to a Princeton Applied Research (PAR, Model 273A) Potentiostat/Galvanostat at Open Circuit Potential (OCP) concerning SCE within a frequency range of 0.1 Hz to 10 kHz with an applied AC signal of 5 mV (RMS) using the single sine technique. Since corrosion phenomena in the soil are strongly pH-dependent.[22] The EIS measurements were carried out to observe the corrosion resistance effect of coating (epoxy/CNTs) on API 5L X65 steel sample in a 2 M hydrochloric acid (HCl) solution. Impedance measurements were also performed to document the epoxy coatings' corrosion after prolonged exposure to the acidic environment. The corrosion protection efficiency (%CPE) values were calculated using Equation 2:[14]

$$(\%\mathrm{CPE}) = 1 - \frac{R_p\,(\mathrm{rawsteel})}{R_p\,(\mathrm{coatedsample})} \tag{2}$$

Where,

$R_{p(\text{raw steel})}$ = the polarisation resistances of the substrate in the absence of the coating nanocomposites

$R_{p(\text{coated sample})}$ = the polarisation resistances of the substrate in the presence of the coating nanocomposites.

3. RESULTS AND DISCUSSION

3.1 Corrosive Soil Parameters

The soil moisture content influenced by rainfall, erosion, and microbial activity, has a synergistic effect on soil aeration. It can be observed in Figure 1 that the moisture content of the soil samples varied in different soil pits, as location 2 contained the highest moisture content (5.73) and the soil samples were confirmed to be clay in the site. The typical pH of soil is within the range of 4 to 10, the results shows pH range from 6.11 to 7.48 which could cause a potential effect on pipeline corrosion. However, due to acid rainfall and acid-producing bacterial organisms in the soil, the average soil pH value is 6.64 as shown in Table 2. This indicates slightly neutral soil that becomes acidic with increasing moisture content. This can be observed in Figure 1 that the higher the moisture content, the higher the pH values. The humic acid generated from organic debris may have contributed to the acidity of the soil environment. The acidic medium aided the soil sample's corrosivity.[23] The results obtained from the average resistivity of soil samples was 167.40 Ω-m. Generally, high soil resistivity will slow down the corrosion activities due to less ionic content flow between the buried metal surface and the corrosive soil environment. The resistivity decreases with increased water content and ion concentration.[24] Therefore, the conductivity and corrosion of the soil are measured by its resistivity. The higher the resistivity value, the lower the corrosion rate, as there is more resistance to the current flow.

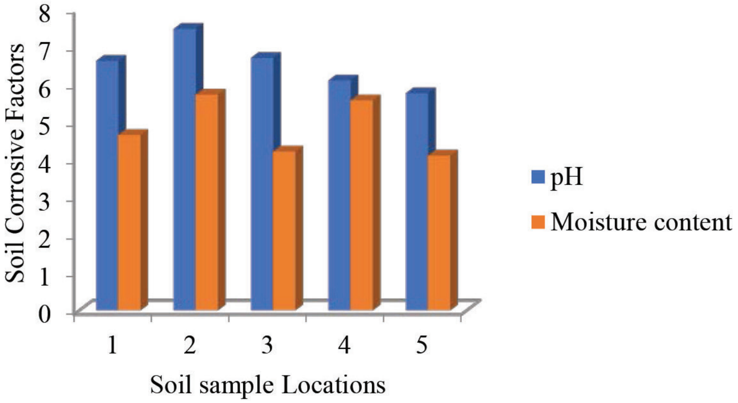

Figure 1: Moisture content and pH as soil corrosive factors in different locations.

The result of the resistivity shows common values. As demonstrated in Table 2, the soil samples' average sulphate level (467.20 mg/kg) had a somewhat corrosive effect. Sulphate is milder in its corrosive actions toward metabolic materials, but it affects concrete and chemically modifies the binding components, producing expansion, cracking and strength loss.[25] Sulphate attacks in reinforced concrete structures can expose rebar to corrosion by other compounds such as chloride. Desiri-Eruteyan et al. found that sulphate concentrations varied from 156.14 mg/kg to 848.50 mg/kg, which contradicts the experimental findings.[26] Because chloride ions are directly involved in electrochemical processes throughout the corrosion process, they are generally detrimental.[27] Table 2 reveals that soil samples' chloride content ranges from 188 mg/kg to 375 mg/kg, indicating corrosive levels.

Thus, the soil may degrade the protective layers that naturally grow on the surface of some metals, exposing the unprotected metal to additional corrosion.

Table 2: Soil corrosivity/aggressivity values.

Soil pits (Location)	pH	Resistivity (Ω-m)	Moisture content	Soil type	Chloride (mg/kg)	Sulphate (mg/kg)	Redox (mV)	Temp (oC)
1	6.63	161	4.66	Clay	188	240	–90	38
2	7.48	193	5.73	Clay	191	242	–87	38
3	6.71	151	4.22	Clay	375	680	–95	38
4	6.11	187	5.58	Clay	372	684	–80	38
5	5.77	145	4.11	Clay	234	490	–95	38
Average	**6.64**	**167.40**	**4.86**	**Clay**	**272**	**467.20**	**–89.40**	38

3.2 Morphology and Composition Analysis of Coated API 5L X65 Steel

The HRSEM cross-section of epoxy, CNTs and epoxy with various CNT ratios coated on steel is observed in Figure 2. The buried uncoated steel developed formation of corrosion scales that shows the corrosive effect of the soil after three months as seen in Figure 2(a). The coated materials' thickness increased with the concentration of CNTs, and the surface protection efficiency rose, disallowing corrosive ion penetration into the substrates. The inclusion of CNTs increased the tensile strength even further. This could be due to the development of bridges between the CNTs and the epoxy resin, which improves bonding. Marriam et al. found that adding CNT to epoxy enhanced the composites' tensile strength and elongation.[28] A fracture and rough texture are visible in the SEM image of the uncoated surface. While the epoxy-covered surface looks to distribute evenly, the CNTs/epoxy surfaces appear to disperse more evenly. Figures 2(d) and (e) show cross-sectional SEM images of 2.5% CNTs/epoxy and 3.5% CNTs/epoxy samples. According to Roy et al. the prominent oxidised CNTs are incorporated and well-dispersed in the epoxy matrix, indicating that CNTs promote uniform distribution in the coating, respectively.[29] The surface of the composite was noticeably smoother, indicating enhanced polymer chain interaction and increased interface toughness. Interactions and covalent bonding make the interface between the epoxy matrix and the CNTs easier.

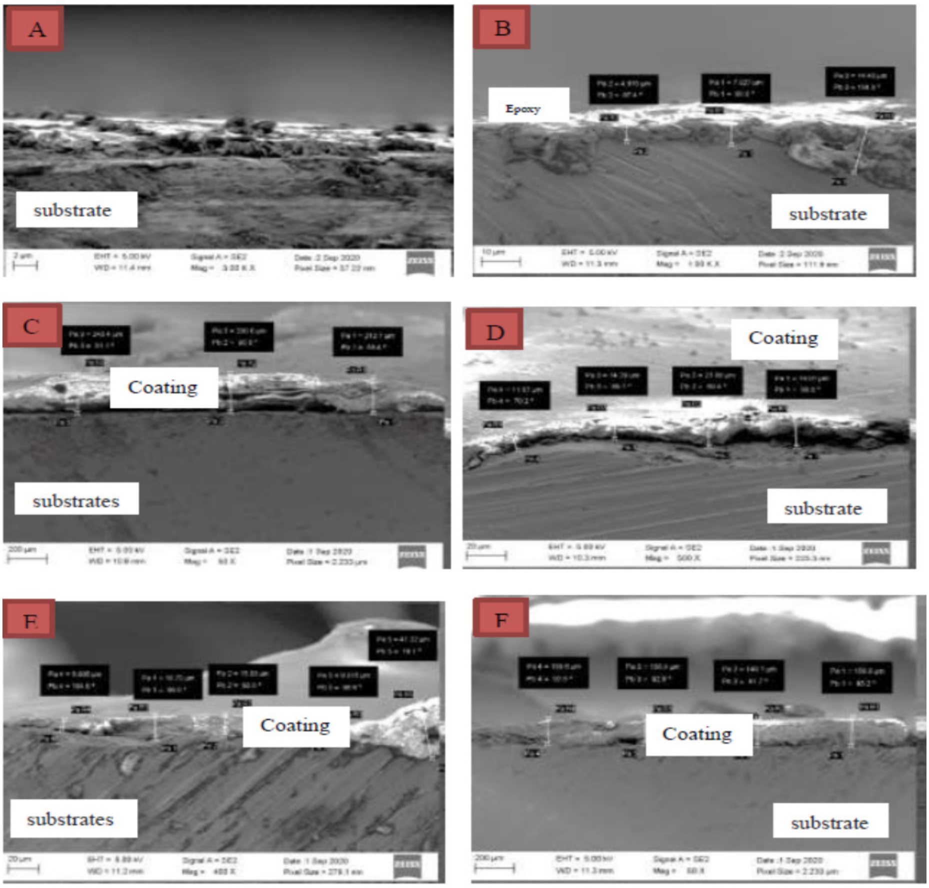

Figure 2: HRSEM cross-sectional micrograph of (a) raw API 5L X65 steel, (b) substrate coated with epoxy resin, (c) 1.5% CNTs, (d) 2.5% CNTs, (e) 3.5% CNTs and (f) 4.5% CNTs.

The elemental makeup of the CNTs/epoxy resin was determined by examining the cross-section of carbon steel covered by an epoxy coating containing CNTs. Figures 3 (a)–(f) show the EDX graphs and their element distribution in the CNTs/epoxy coating. Carbon (C), Oxygen (O) and Iron (Fe) peaks appeared when CNTs/epoxy resin was coated on API 5L X65 steel. However, only these components above were found at various atomic percentages in coated steel with distinct CNTs ratios contained in epoxy resin.

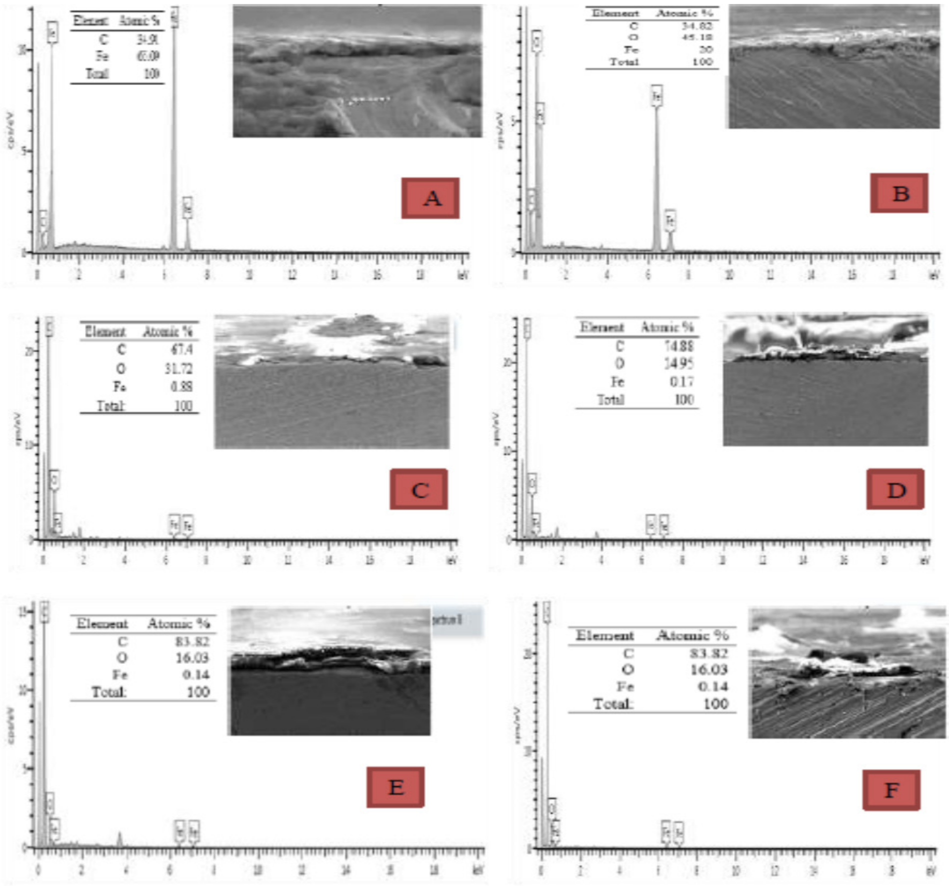

Figure 3: EDX analyses of (a) raw steel, (b) steel substrate coated with epoxy resin, (c) 1.5% CNTs, (d) 2.5% CNTs, (e) 3.5% CNTs and (f) 4.5% CNTs

The Uncoated steel, on the other hand, has peaks of carbon C, O and Fe, with an atomic percentage of Fe higher than coated API 5L X65 steel. However, it's reasonable to expect some CNT/epoxy resin to accumulate at the steel/coating contact. The findings observed in HRSEM pictures of CNTs/epoxy-coated steel confirm this idea. The coated substance reacts with the Fe^{2+} ion to generate a complex compound that protects the carbon steel. The CNTs/epoxy resin will play a key part in the barrier effect and operate as a corrosion inhibitor at the mild carbon steel/coating interface, according to the surface study. The comparison of HRSEM images of CNTs/epoxy resin at different ratios, displayed in Figure 4 (a)–(d), at the same magnification, demonstrates the changes at varied concentrations of CNTs. Variation in surface morphology was seen at high CNT concentrations. The big smooth regions of resin appear to fade away with time, leaving agglomerated particles. The agglomerated CNTs/epoxy resin complexes appear to become clogged with each other.

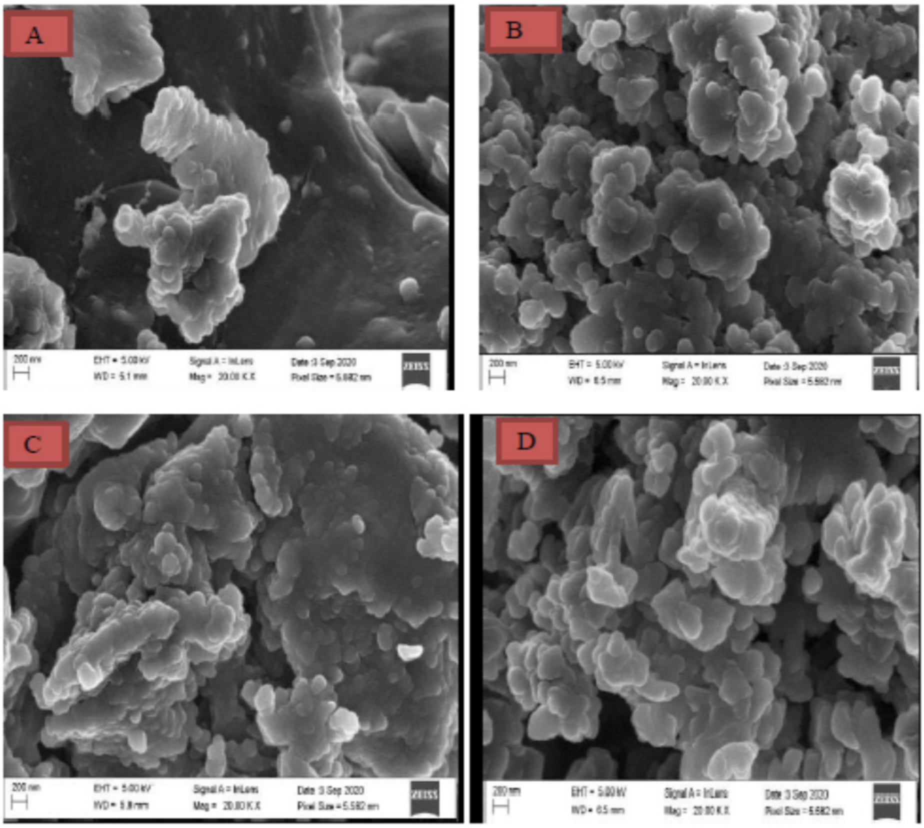

Figure 4: HRSEM cross-sectional micrograph of (a) 1.5% CNTs, (b) 2.5% CNTs, (c) 3.5% CNTs and (d) 4.5% CNTs.

3.3 Tensile strength and Hardness Properties of Coated Steel

The tensile strength and modulus tests show that the CNTs boost epoxy resin's tensile strength and tensile modulus. The inclusion of 4.5% CNT had the greatest impact on the composite's mechanical strength, as presented in Table 3. The agglomerates in the matrix act as big particles, enhancing the resin matrix's network structure and stability. Furthermore, the reinforcing CNTs were confined in the void area of the polymer matrix, substantially reducing the epoxy resin volume percentage. The epoxy resin made without CNTs had lower tensile strength and young modulus. The sample's lack of interfacial bonding could explain this behaviour, resulting in high-stress concentration and low stress distribution uniformity.[30]

Furthermore, Table 3 displays the hardness of epoxy resin and CNTs/epoxy resin composites. The use of CNT appears to increase the hardness variability of composite samples greatly. The dispersion of CNTs in the polymer, which impacts the final nanocomposite properties, could be due to the great range of hardness which is in line with the findings of Francisco et al.[31] CNTs/epoxy property hardness as a function of CNTs loading concentration is higher than epoxy resin hardness. The high level of hardness in CNTs/epoxy matrix could be due to overlaping and stacking, which lowers polymer molecule flow, enhancing scratch resistance and making the material more resistant to deformation. The hardness of materials is determined by the type of forces that bind atoms in the material. Therefore, the strong connections with the CNTs or MWCNTs and epoxy resin interface strongly boost the mixture's coherence, resulting in high hardness and strength properties of the nanocomposite.[32]

Table 3: Mechanical properties of epoxy and epoxy with different CNTs content.

Sample	**Tensile strength (GPa)**	**Tensile modulus (GPa)**	**Hardness (HV)**
1.5 %epoxy	2.08	16.20	11.40
1.5 %CNTs/epoxy	3.17	21.74	12.02
2.5 % CNTs/epoxy	4.63	23.50	12.36
3.5 % CNTs/epoxy	4.90	24.10	13.05
4.5 % CNTs/epoxy	5.81	25.64	13.74

3.4 Moisture Test

The results of the moisture for buried uncoated and coated samples for a year are presented in Figure 5. S1 represents 1.5% epoxy, S2 represents 1.5% CNTs/epoxy, S3 represents 2.5% CNTs/epoxy, S4 represents 3.5% CNTs/epoxy, while S5 represents 4.5% CNTs/epoxy, respectively. From the first three to the twelfth month, gradual moisture absorption was detected in uncoated steel samples (S1). On the other hand, all of the coated samples (S2 to S5) showed no substantial moisture gain. The stiff reinforcement in the composites may impact the structure and molecular interaction inside the composite under wet conditions, resulting in the non-absorption of the water molecule. Furthermore, the water molecule has a considerable affinity for the uncoated sample due to steel's electrophilic character, whereas it has less effect with the hydrophobic CNTs.

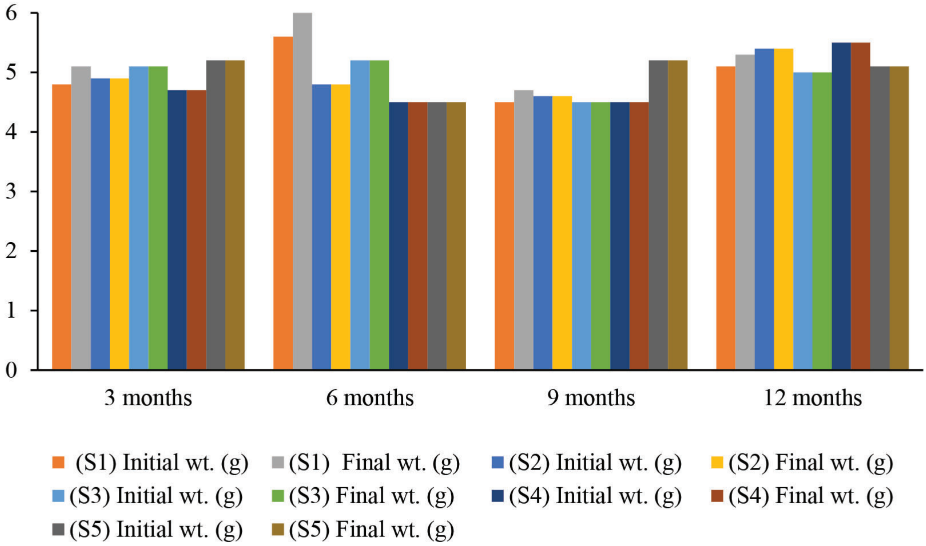

Figure 5: Moisture test of buried samples for different months.

3.5 EIS Measurement

In a 2 M HCl solution, the effect of varying concentrations of CNTs covering material with epoxy on carbon steel corrosion prevention was investigated. Coating the surface of metals limits the movement of electrons or ions, which is thought to stop the corrosion reaction.[33] As a result, the coating's electrical properties are important for the layer's capacity to provide enough corrosion protection and operate as a perfect electrical and chemical barrier for the underlying substrate. To understand corrosion behavior, electrical parameters can be fitted into equivalent models.

The simplest electrical equivalent circuit (EEC) to depict a coating and corroding metal is the Randles circuit model.[34] On the other hand, the coated sample might be well matched using a Randles circuit with two-time constants as shown in Figure 6.

The electrical equivalent circuit is made up of a solution resistance element (Rs) in series with coating capacitance (Cc), and a coating pore resistance (Rpo) that reflects the resistance of ionic conduction channels that pass through the coating. Coating resistance, a constant capacitance phase element double layer (CPEdl) representing the passive film's capacitance double layer (Cdl), and a charge transfer element low-frequency zone (Rct) across the passive film are all terms used to describe this (corrosion resistance). Rct and Cdl are components for studying the corrosion reaction of coating samples, as can be seen. Better charge transfer resistance has been linked to higher model corrosion resistance, and Cdl follows the inverse pattern.[35]

The sum of the two series resistors, Rs and Rpo, defines the impedance of the Randles circuit. In both the high and low-frequency ranges, the Randles circuit acts essentially as a resistor. At intermediate frequencies, however, the capacitor's impedance is critical, and the cell serves as a capacitor. As a result, the imaginary component grows in importance, the phase angle approaches –90°, and linearly, the cell impedance becomes frequency-dependent (on a log-log scale).

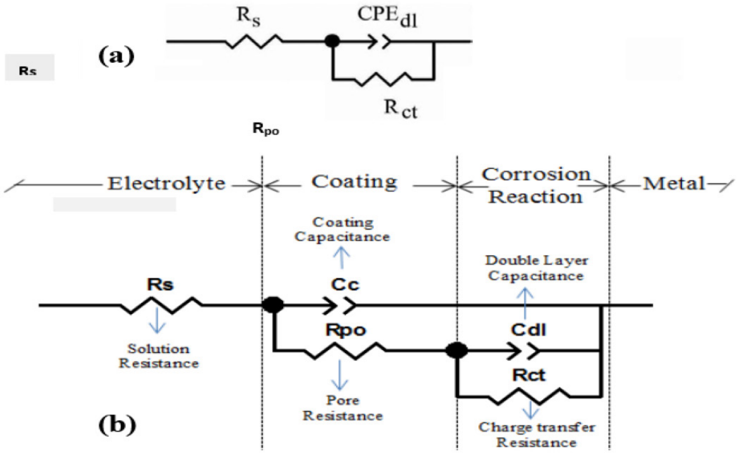

Figure 6: Coating electrical equivalent circuit model with traditional circuit elements for (a) uncoated and (b) coated samples.

The interface between this pocket of solution and bare metal is treated as a double-layer capacitance, Cdl in tandem with a kinetically controlled charge transfer reaction element represented by the charge transfer resistance in one of the interpretations of this model. It's also known as polarisation resistance (Rp), which refers to the resistive corrosion product layer on the metal plate and Rct, which is inversely proportional to the rate of corrosion.[34]

The experimental impedance spectra fit Nyquist graph with Z-simp software as shown in Figure 7. For three potentials, the imaginary component of impedance is plotted against the fundamental component in the Nyquist plane as a function of decreasing frequencies in Figure 7. The data is also displayed versus the logarithm frequency in phase angle i.e., arctan (–Z /Z'). As a result, the Z" denotes imaginary impedance, while the Z' denotes actual impedance. Table 4 presents the obtained experimental data, which includes elements of the proposed equivalent circuit such as Rs, Rpo, Rct, Cc, CPEdl and Rp (polarisation resistance of the metal, which is Rpo+ Rct). According to the resistance analysis, the coating's water and acid solution resistances are significantly better than those of raw steel and epoxy coating alone. Furthermore, the electrochemical impedance spectroscopy test revealed that the layer protected metals from corrosion better than epoxy.

Table 4: Electrochemical impedance spectroscopy parameters.

Coatings	**R_S (Ωcm^2)**	**Rpo (KΩcm^2)**	**Rct (KΩcm^2)**	**CPE_{dl} (μF/cm^2)**	**n_{dl}**	**CPE%**
Raw Steel (no coating)	26.8	0.06	0.384	125.04	0.89	
Epoxy only	29.06	0.251	0.809	87.71	0.75	63.21
Epoxy + 1.5CNTs	168.9	1.513	3.123	63.61	0.90	91.59
Epoxy + 2.5CNTs	178.2	1.723	4.323	52.93	0.91	93.55
Epoxy + 3.5CNTs	185.7	2. 324	5.002	44.27	0.92	94.68
Epoxy + 4.5CNTs	163.2	1.125	2.069	81.34	0.90	87.79

The creation of an adsorption layer on the steel surface can be attributed to increased Rct values as the epoxy coating concentration increases. The adsorbed surface at the electrode surface acts as a barrier to charge transport demonstrating its anti-corrosive property. The high-frequency area of the EIS spectrum relates to coating behaviour, while the low-frequency region corresponds to corrosion reaction.[36] The capacitance component is assumed to be the corrosion's double-layer capacitance at the steel surface. Furthermore, in the high-frequency region, the resistances in the spectrum are considered to be coating resistance. In contrast, a charge transfer resistance correlates to corrosion reaction in the low-frequency zone.

The Nyquist plot that shows an incomplete/partial arc in the high-frequency band, indicating low charge-transfer resistance, followed by a linear line in the low-frequency range, indicating a low charge-transfer resistance as shown in Figure 7. The resistance of the coatings was shown in the high-frequency region, whereas the charge transfer resistance was demonstrated in the Rct. Samples in 2 M HCl solution have the following charge transfer resistance. The corrosion protection efficiency rises with increasing CNT concentrations, peaking at 94.68% for 3.5 g/l CNTs, demonstrating the greatest performance of all the coatings produced. Further increases in CNT concentration (4.5 g/l) result in lower corrosion resistance. It has been reported that the decrease in strength at higher CNT or MWCNT concentrations indicates agglomeration defect behaviour of the CNTs due to local CNTs differences and the impairment of the charge transfer to the epoxy resin matrix.[32]

The n_{dl} values which is a parameter adjustable from 0.5 to 1 and is calculated from the slope of log|Z| vs. log|f| from Bode plot. The values and charge transfer resistanceincreased with increasing CNT concentration before decreasing at 4.5 g/l. CPEdl, on the other hand, was shown to have an inverse trend. As previously indicated, increasing the CNT concentration to 3.5 g/l enhanced the amount of CNTs integrated into the composite coating. As a result, the charge transfer resistance was improved due to the ease of chemical passivation and the rapid creation of a thicker P-rich film with poor ionic conductivity qualities that protects the coating's active surface from solution and corrosive substances.[13]

Deposition of nanoscale CNTs filled the crevices, gaps, and micron holes in the coating, reducing surface and structural defects, and increasing the incorporated CNTs content, resulting in the formation of a denser and more homogeneous layer, resulting in a decrease in CPEdl and an increase in n_{dl} values.[37] The porosity and surface inhomogeneity of the coating can be linked to CPEdl and n_{dl} values, according to Alishahi et al.[13] The porosity and fault density of the composite layer tend to rise as the CNT concentration increases. As a result, the n_{dl} value has risen while the CPEdl value has fallen.

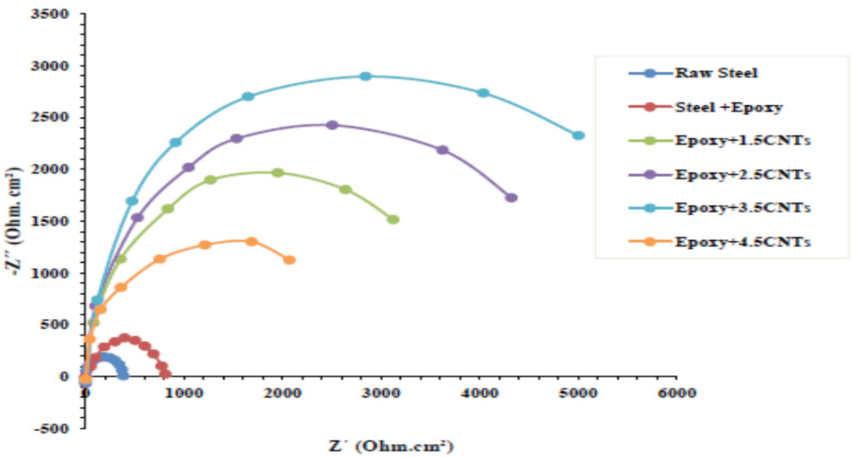

Figure 7: Nyquist plots of carbon steel coated with epoxy and different concentrations of CNTs.

The Bode phase plot of steel, epoxy coating, and epoxy coating with varying amounts of CNTs following immersion in HCl solution is depicted in Figure 8. The high phase angle at the medium frequency region signifies an excellent barrier property of the surface coating and corresponds to less corrosive ions being in contact with the metal surface, whereas at the large modulus, the plot shows peaks for all samples in the low-frequency region that discloses the enhancement of corrosion resistance.[35]

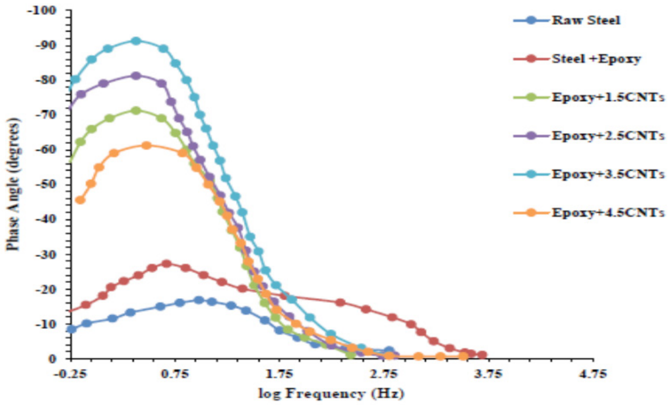

Figure 8: Bode plot for carbon steel coated with epoxy and different concentrations of CNTs.

The phase angle aperture increases after CNTs are added to the epoxy coating, as shown in the graph. These confirmed Niquist’s findings, suggesting that the corrosion resistance of the coating was determined to be highest at a concentration of 3.5 g/l CNTs. By filling the coating’s porosities, gaps, cracks and micron holes, adding CNTs to the epoxy coating reduces the number of surfaces and structural flaws. The raw steel had a tiny phase angle, and the aperture of the phase angle was lowered because the surface layer couldn’t adequately cover the substrate, which is consistent with Dieleman et al.’s findings.[38] As a result, a coating incorporating CNTs effectively delays electrolyte penetration and improves the coating’s barrier effectiveness. In addition, the results reveal that the coated steel is more stable in a corrosive environment like acidic soil than pure epoxy coating.

4. CONCLUSION

The HRSEM cross-section of epoxy, CNTs, and epoxy with various CNTs coated on API 5L X65 steel is investigated. The thickness of the coated materials on the steel increased due to the increased viscosity of the solution with a high amount of CNTs, leading to more infiltration of the solution into the films. The results of the tensile strength, hardness, and tensile modulus of epoxy resin with CNTs increase with CNTs. It was found that adding 3.5% CNTs has the best effect on the mechanical strength of the composite. The EIS analysis reveals that nanocomposite coatings had significantly excellent conductors. It is attributed that coating surface hydrophobicity is enhanced by adding CNTs.

5. ACKNOWLEDGEMENTS

This research was funded by the tertiary education trust fund (TETFUND), Nigeria, with grant number TETFUND/FUTMINNA/2019/B7/13.

6. REFERENCES

1. Bhardwaj A. (2017). Petroleum fluids properties and production schemes: Effect on corrosion. In A. M. El-Sherik (Ed.). *Trends in Oil and Gas Corrosion Research and Technologies*. Swaston, UK: Woodhead Publishing, 31–52. https://doi.org/10.1016/B978-0-08-101105-8.00002-4
2. Gupta, P. et al. (2016). Metal matrix nanocomposites and their application in corrosion control. *Adv. Nanomater.*, 79, 231–246. https://doi.org/10.1007/978-81-322-2668-0_6
3. Sadhya S. G. (2017). Modelling of Corrosion Electrochemistry in Sweet Environments Relevant to Oil and Gas Operations. PhD diss., University of Manchester United Kingdom.
4. Gu, B. E. et al. (2018). Effects of multiwall carbon nanotube addition on the corrosion resistance and underwater acoustic absorption properties of polyurethane coatings. *Prog. Org. Coat.*, 121, 226–235. https://doi.org/10.1016/j.porgcoat.2018.04.033
5. Ding, J. H. et al. (2018). A long-term anticorrosive coating through graphene passivation. *Carbon*, 138, 197–206. https://doi.org/10.1016/j.carbon.2018.06.018
6. Mahidashti, Z. et al. (2018) Screening the effect of chemical treatment of steel substrate by a composite cerium-lanthanum nanofilm on the adhesion and corrosion protection properties of a polyamide-cured epoxy coating; Experimental and molecular dynamic simulations. *Prog. Org. Coat*, 114, 188–200. https://doi.org/10.1016/j.porgcoat.2017.10.020
7. Ahmadi, Z. (2019). Nanostructured epoxy adhesives: A review. *Prog. Org. Coat.*, 135, 449–453. https://doi.org/10.1016/j.porgcoat.2019.06.028

8. Deyab, M. A., & Awadallah, A. E. (2020). Advanced anticorrosive coatings based on epoxy/functionalized multiwall carbon nanotubes composites. *Prog. Org. Coat.*, 139, 105423. https://doi.org/10.1016/j.porgcoat.2019.105423
9. Liu, S. et al. (2018). A review of extending performance of epoxy resins using carbon nanomaterials. *Compos. B Eng.*, 136, 197–214. https://doi.org/10.1016/j.compositesb.2017.08.020
10. Han, S. et al. (2019). Mechanical, toughness and thermal properties of 2D material-reinforced epoxy composites. *Polymer*, 184, 121884. https://doi.org/10.1016/j.polymer.2019.121884
11. Wu, S. et al. (2017). Aligning carbon nanofibers in glass-fiber/epoxy composites to improve interlaminar toughness and crack-detection capability. *Compos. Sci. Technol.*,152, 46–56. https://doi.org/10.1016/j.compscitech.2017.09.007
12. Hanaei, H. et al. (2016). Highly efficient antireflective and self-cleaning coatings that incorporate carbon nanotubes (CNTs) into solar cells: A review. *Renew. Sustain. Energy Rev.*, 59, 620–635. https://doi.org/10.1016/j.rser.2016.01.017
13. Alishahi, M. et al. (2012). The effect of carbon nanotubes on the corrosion and tribological behavior of electroless Ni–P–CNT composite coating. *App. Surf. Sci.*, 258(7), 2439–2446. https://doi.org/10.1016/j.apsusc.2011.10.067
14. Abdulrahman, M. A. et al. (2017). Effect of coating mild steel with CNTs on its mechanical properties and corrosion behaviour in acidic medium. *Adv. Nat. Sci. Nanosci. Nanotechnol.*, 8, 015016. https://doi.org/10.1088/2043-6254/aa5cf8
15. Kasar, A. K. et al. (2020). Corrosion performance of nanocomposite coatings in moist SO2 environment. *Int. J. Adv. Manu. Technol.*, 106, 4769–4776. https://doi.org/10.1007/s00170-020-04949-z
16. Janaki, G. B., & Xavier J. R. (2020). Effect of indole functionalized nano-alumina on the corrosion protection performance of epoxy coatings in marine environment, *J. Macromol. Sci. A.*, 57(10), 691–702. https://doi.org/10.1080/10601325.2020.1761831
17. Awadallah, A. E. et al. (2014). Impact of group VI metals addition to Co/MgO catalyst for non-oxidative decomposition of methane into COx-free hydrogen and carbon nanotubes. *Fuel*, 129, 27–36. https://doi.org/10.1016/j.fuel.2014.03.038
18. Buhari, S. A. et al. (2019). Synthesis of carbon nanotubes using catalytic chemical vapour decomposition of acetylene over Co-Mo bimetallic catalyst supported on magnesia. *Nigerian J. Eng. Appl. Sci.*, 6(1), 46–57.
19. Lobiak, V. E. et al. (2020). *Effect of Co-Mo catalyst preparation and CH4/H2 flow on carbon nanotube synthesis. Fullerenes Nanotubes and Carbon Nanostructures*, 28(9), 1–9. https://doi.org/10.1080/1536383X.2020.1749051
20. Raza, M. A. et al. (2016). Production of carbon nano-tubes via CCVD method and their corrosion protection performance in epoxy based coatings. Paper presented at *IOP Conference Series: Materials Science and Engineering IOP Publishing*, National Centre for Physics, Islamabad, Pakistan, 12–16 October 2015, 146(1), 012021. https://doi.org/10.1088/1757-899X/146/1/012021
21. Isakhani Zakaria, M. et al. (2019). Evaluation of corrosion behaviour of Pb-Co3O4 electrodeposited coating using EIS method. *Corros. Sci.*, 157, 472–480. https://doi.org/10.1016/j.corsci.2019.06.023

22. El-Reedy, M. A. (2020). Corrosion protection. *Offshore Structures.* 359–417. https://doi.org/10.1016/B978-0-12-816191-3.00006-7
23. Soriano, C., & Alfantazi, A. (2016). Corrosion behavior of galvanized steel due to typical soil organics. *Constr. Build. Mater.*, 102(1), 904–912. https://doi.org/10.1016/j.conbuildmat.2015.11.009
24. Wasim, M. et al. (2018). Factors influencing corrosion of metal pipes in soils. *Environ. Chem. Lett.*, 16(3), 861–879. https://doi.org/10.1007/s10311-018-0731-x
25. Moore. A. (2019). Effect of oxygen availability on the corrosion rate of reinforced concrete in marine exposure zones: Inference from site and lab studies. Masters diss., University of Cape Town, South Africa.
26. Odesiri Eruteyan, E. A. et al. (2020). The potential corrosiveness of soil physico-chemical properties on pipelines. *J. Sci. Res. Rep.*, 26(3), 99–108. https://doi.org/10.9734/jsrr/2020/v26i330241
27. Xia, J. et al. (2019). Numerical simulation of steel corrosion in chloride contaminated concrete. *Constr. Build. Mater.*, 228, 116745. https://doi.org/10.1016/j.conbuildmat.2019.116745
28. Marriam, I. et al. (2018). Synergistic effect of CNT films impregnated with CNT modified epoxy solution towards boosted interfacial bonding and functional properties of the composites. *Compos. Part A Appl. Sci. Manuf.*, 110, 1–10. https://doi.org/10.1016/j.compositesa.2018.04.011
29. Roy, S. et al. (2018). Effect of carbon nanotube (CNT) functionalization in epoxy-CNT composites. *Nanotechnol. Rev.*, 7(6), 475–485. https://doi.org/10.1515/ntrev-2018-0068
30. Panchagnula, K. K., & Kuppan, P. (2018). Improvement in the mechanical properties of neat GFRPs with multi-walled CNTs. *J. Mater. Res. Technol.*, 365, 1–11 https://doi.org/10.1016/j.jmrt.2018.02.009
31. Francisco, W. et al. (2015). Functionalization of multi-walled carbon nanotube and mechanical property of epoxy-based nanocomposite. *J. Aerosp. Technol. Manag.*, 7(3), 289–293. https://doi.org/10.5028/jatm.v7i3.485
32. Pekturk, H. Y. et al (2022). Evaluation of the effect of MWCNT amount and dispersion on bending fatigue properties of non-crimp CFRP composites. *Eng. Sci. Technol. Int. J.*, 34, 1–11. https://doi.org/10.1016/j.jestch.2021.101081
33. Hussain, M. S. (2018). Synthesis of bulk nanostructured materials by high-speed turbulent flow—a method of electrodepositing nanocrystalline nickel. In C. M. Hussain (Ed.). *Nanomaterials in Chromatography*. Amsterdam: Elsevier, 55–88. https://doi.org/10.1016/B978-0-12-812792-6.00003-0
34. Hernández, H. H. et al. (2020). Electrochemical Impedance Spectroscopy (EIS): A review study of basic aspects of the corrosion mechanism applied to steels. In Marwa El-Azazy et al. (Eds.). *Electrochemical Impedance Spectroscopy.* Vienna: Intechopen, 1–35. https://doi.org/10.5772/intechopen.94470
35. Bakhsheshi Rad, H. R. et al. (2016). Introducing a composite coating containing CNTs with good corrosion properties: characterization and simulation. *RSC Adv.*, 6(110), 108498–108512. https://doi.org/10.1039/C6RA24222G

36. Indira, K., & Nishimura, T. (2016). Corrosion resistance of epoxy-coated 3% Cr steel in saline environment measured using EIS and SECM. *Int. J. Electrochem. Sci*., 11, 419–431.
37. Chandresh, A. et al. (2021). Insights in the ionic conduction inside nanoporous metal-organic frameworks by using an appropriate equivalent circuit. *Materials*, 14, 4352. https:// doi.org/10.3390/ma14164352.
38. Dieleman, C. D. et al. (2018). Long-term active corrosion protection of damaged coated-aa2024-t3 by embedded electrospun inhibiting nanonetworks. *Adv. Mater. Interf.*, 5(12), 1800176. https://doi.org/10.1002/admi.201800176